



**COVER PAGE**

***Document downloaded by @DAEL***

***Wed May 27 17:33:19 2026***

***For personal use***

When automatic English translation is provided, only the original document is authentic.

The EAA cannot be held responsible of any translation error

Bibliographical reference

*Thermally Stimulated Acoustic Energy Shift in Transformer Oil*, J. Petras, J. Kurimsky, J. Balogh, R. Cimbala, J. Dzmura, B. Dolnik and I. Kolcunova, *Acta Acustica* **vol. 102** (Number 1), 2016, pp. 16-22

DOI

<https://doi.org/10.3813/AAA.918920>

# Thermally Stimulated Acoustic Energy Shift in Transformer Oil

J. Petras, J. Kurimsky, J. Balogh, R. Cimbala, J. Dzmura, B. Dolnik, I. Kolcunova  
Department of Electric Power Engineering, Technical University of Kosice, Masiarska 74,  
04001 Kosice, Slovakia. [jaroslav.petras, juraj.kurimsky, jozef.balogh, roman.cimbala,  
jaroslav.dzmura, bystrik.dolnik iraida.kolcunova]@tuke.sk

## Summary

In this paper, partial discharge acoustic emission waveform data collected in high voltage transformer oil are analysed over certain temperature range. Analytical model and method of thermally stimulated acoustic energy shift calculation is proposed. It allows to uncover the effect of acoustic emission energy shift over the frequency spectra due to the change of fluid temperature. The variations in the received acoustic waveform data have been analyzed. Continuous partial discharge generation was provided by Böning model. The analytical model has been verified by experimental data analysis. In the field of non-destructive testing of high voltage power devices it provides a new understanding of the temperature role on interpretation of partial discharges generated acoustic emission.

PACS no. 43.20.Hq, 43.35.Zc, 43.58.Gn, 43.60.Hj, 43.60.Jn, 52.80.Wq

## 1. Introduction

The acoustic emission measurement is a powerful tool in many industrial branches. It is used as a maintenance utility as well as tool for non-destructive testing. The technique is based on the phenomena when aging of electrical insulating system is accompanied by acoustic effects [1, 2, 3, 4].

High voltage devices use to have very complicated shape in terms of the electrode and dielectric barrier system configuration. The dielectric barrier system often consists of multi-component insulation and therefore it requires high care during manufacturing process [5, 6, 7].

The crucial influence on high voltage electric device lifetime and reliability has its insulating system. There are various methods for insulating system quality measurement. In a lot of maintenance utilities, complex parameters measured on the device and describing partial discharges (PD) are used for its life-time prediction. Partial discharges are powerful indicator of insulating system pre-breakdown status [8, 9, 10].

Various direct and indirect methods of PD measurement are well-known and widely used, e.g. in expert systems [11, 12, 13]. Acoustic emission measurement takes a special place among them because of its partial discharge allocation capabilities [14, 15]. Not so widely used and researched way of the partial discharge acoustic emission data exploitation is its usage in PD type recognition

based on the waveform shape [16]. It can be useful to uncover the real power of this method mainly for the non-destructive testing purposes, when the similarities in the acoustic emission signal generated by the same type of PD or same type of defect in dielectric material can be detected.

The information on several PD properties are projected to acoustic waveform shape. However, in the electric power system, there are a lot of factors related to it. In general, they cause the loss of the PD information. They have complex constructions and they use the materials of different physical properties.

Acoustic method of discharge activity measurement used in electric power device diagnostics is based on PD acoustic emission measurement. So far it is used mainly for the defective dielectric area allocation [17]. Three or more sensors have to be used for this purpose.

In the loaded high voltage power transformer the temperature of the insulating oil is assumed to be a global parameter for whole system although there are in this case negligible thermal gradients. The temperature can be considered as a global parameter. The following experiment is coupled with the change of the global temperature.

The environment temperature is the global parameter refining the spatio-temporal model patterns. Therefore it is important to know how the temperature of the insulating system changes partial discharge acoustic emission waveform [18, 19]. In following sections we propose the analytical model and experimental verification of this temperature problem.

---

Received 05 February 2015,  
accepted 12 November 2015.

## 2. Theoretical analysis

### Physical background

When partial discharge appears, a part of the electric energy changes to mechanical energy and the area in dielectric material with PD becomes consequently a source of mechanical waves. The frequency range of this wave motion lies in acoustic or supersonic bandwidth and can be sensed by acoustic sensors.

Let us suppose that only pressure waves can propagate in a liquid, because the viscosity and shear forces are small. The velocity of sound in liquids varies from 900 to 2000 m/s. The velocity of sound in most liquids decreases almost monotonically as the temperature decreases too i.e. by 2 to 6 m/s per °C with water as an exception [17]. In liquids the absorption of acoustic energy increases with the square of frequency. The losses are proportional too and they are dominated by the viscosity.

We can mathematically describe and express a travelling sound by equation (1) [20],

$$\xi(x, t) = \xi_0 \cdot e^{-\alpha x} \cdot e^{i(\omega t - k \cdot x)}, \quad (1)$$

where the  $k$  denotes the wave number which depends on the frequency for fluids and gasses [21] and

$$\alpha = \frac{\omega^2 \cdot \nu}{6 \cdot c^3}. \quad (2)$$

Then (1) can be written as in (3) [20],

$$\xi(x, t) = \xi_0 \cdot e^{-\frac{2(\pi f)^2 \cdot \nu}{3 \cdot c^3} \cdot x} \cdot e^{i(\omega t - k \cdot x)}. \quad (3)$$

The parameter  $c$  denotes the acoustic velocity of wave in oil and it is measured in m/s. It is approximately 1400 m/s at temperature 0°C. The parameter  $\xi_0$  denotes the static value or amplitude of wave.  $\nu$  denotes kinematic viscosity of liquid where sound waves occur, in our case kinematic viscosity of the transformer oil. It is the ratio of the dynamic viscosity  $\mu$  to the density of the fluid  $\rho$ . It strongly depends on temperature of oil, which can be expressed by (4), which is an empiric model equation [22, 20],

$$\nu = \frac{\nu_0}{1 + aT + bT^2}. \quad (4)$$

In (4)  $T$  denotes the temperature of oil in °C and  $\nu_0$  denotes kinematic viscosity at 0°C. Usual values for  $\nu_0$  for transformer oils are about 66 cSt, which is also our case. Parameters  $a$  and  $b$  take values 0.097965 and 0.0014588 respectively and are empirically stated for this kinematic viscosity temperature model in [22].

Taking this into consideration we can rewrite equation (3) like in (5) [20],

$$\xi(x, t) = \xi_0 \cdot e^{-\frac{2(\pi f)^2 \cdot \nu_0}{3 \cdot c^3 (1 + aT + bT^2)} \cdot x} \cdot e^{i(\omega t - k \cdot x)}. \quad (5)$$

The dependence on the temperature is not assumed. Equation (6) describes wave amplitude [20],

$$E = \xi_0 \cdot e^{-\frac{2(\pi f)^2 \cdot \nu_0}{3 \cdot c^3 (1 + aT + bT^2)} \cdot x}. \quad (6)$$

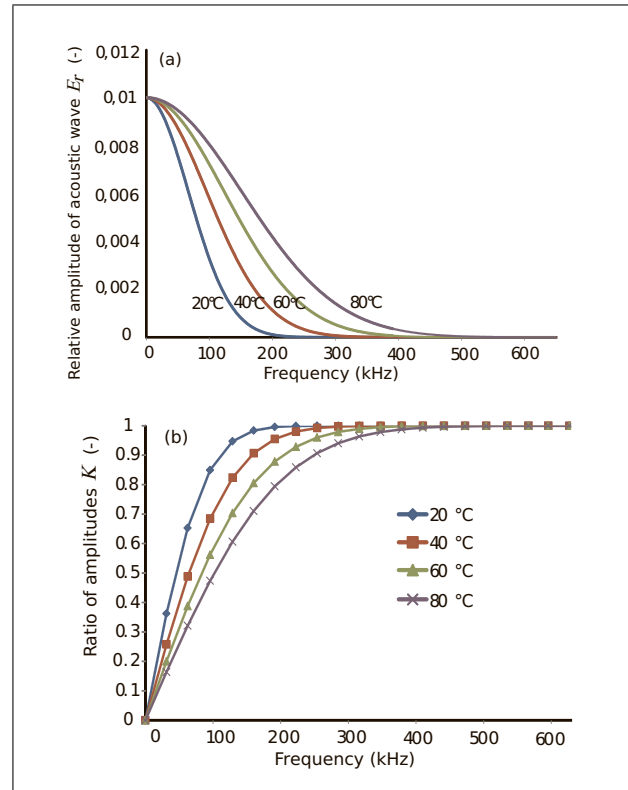


Figure 1. a) The dependence of acoustic wave amplitude on temperature in modelled situation; b) The ratio of frequency amplitude sum in 30kHz bands at temperatures 20°C, 40°, 60° and 80° respectively.

### Feature extraction

In following section, let us assume, for the acoustic velocity, any variation with temperature has not been taken into account.

Equation (6) expresses the relationship of acoustic wave amplitude and temperature. This dependence can be seen in Figure 1, where relative values  $E_r(f)$  of this amplitude are depicted.

$$E_r(f) = E(f)/\xi_0. \quad (7)$$

Acoustic waves propagating in liquids follow the laws of fluid mechanics. The propagation of an acoustic wave is associated with an acoustic energy [21].

In the following text we propose how to quantify the acoustic energy shift in the frequency domain due to temperature changes, based on the assumption of kinematic viscosity thermally initiated changes. Due to intended application of the Fourier transform, formally, the frequency band from 0 MHz upto 1 MHz was divided into 32 sub-bands of 31.250 kHz bandwidth.

The frequency domain analysis was performed on a subset of 1024 waveforms by means of Fourier transform. This procedure was repeated for each of examined temperatures, i.e. 20°C, 40°C, 60°C and 80°C which represent several basic thermal modes of high voltage transformer under operation.

Because of big amount of measured waveforms per second respectively per each measured temperature, we have created a waveform template. The waveform template calculation method is based on the statistical methods. It been described in [23]. Again, we applied the Fourier transform on these template waveforms and we calculated their spectra.

Inspired by [24], the dominant frequencies have been adapted as frequencies in specific frequency bands with spectral amplitude coefficient values at least 5 times greater than the values of other spectral components.

To compare the portion of signal spectrum amplitude components the coefficient  $K$  was calculated as the ratio of the sum of frequency amplitudes in given sub-bands and the sum of frequency amplitudes in the whole spectrum,

$$K_i = \frac{\sum_0^{i \cdot 31.25 \text{kHz}} E}{\sum_0^{1 \text{MHz}} E}, \quad (8)$$

where index  $i = 1, 2, 3, \dots, 32$ .

The proposed analytical model at several temperature modes yields the result as it is shown in Figure 1b. As can be seen, the kinematic viscosity model clearly shows the acoustic energy shift to higher frequencies with rising temperature.

In this manner, the feature extraction gives a set of discrete values of dominant frequencies or sub-bands values of parameter  $K_i$  as defined in equation (8).

### 3. Experiment

For reference purposes along with acoustic method also galvanic PD measurement was used.

For this method MTE3 PD detection device was used which receives signal from measurement impedance and serves as a referential monitor for PD activity presence. The experiment was set up according to the block diagram depicted in Figure 2.

High voltage generated by HV TR high voltage transformer was connected to sample under examination and it was regulated by  $U_{\text{Reg}}$  to achieve discharge activity on tested sample upon continuously increasing high voltage until first PD occur. The signal was looped through to the digital oscilloscope. The voltage was increased up to the value when discharge activity appeared to be stable.

Simultaneously acoustic measurement was applied. The instrumentation and data acquisition software of Physical Acoustic was used. Three timing parameters have been used to identify waves in the related environment: the peak definition time (PDT), the hit definition time (HDT), the hit lockout time (HLT). In this way the problems related to reflections, wave-modes in steel plates, etc have been solved. More information on this topic can be found in [25].

The transformation of acoustic wave to electric signal was made in the crystal transducers. We used a pair of resonant type crystal transducers R15I-AST with built-in pre-amplifier. This sensor type works with 40 dB gain, which

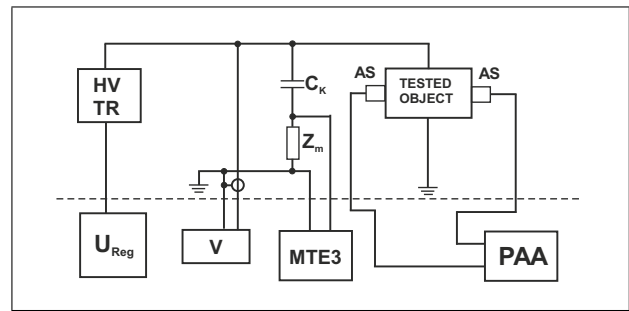


Figure 2. Block diagram for partial discharge activity measurement by acoustic and galvanic method. HV TR – High Voltage Transformer.  $U_{\text{Reg}}$  – Voltage Regulation. V – Voltmeter. MTE3 – Partial discharge measuring device. AS – Acoustic Sensor. PAA – Physical Acoustic PCI-2 recording card and data acquisition software.  $Z_m$  – Measurement impedance.  $C_k$  – Coupling capacitance.

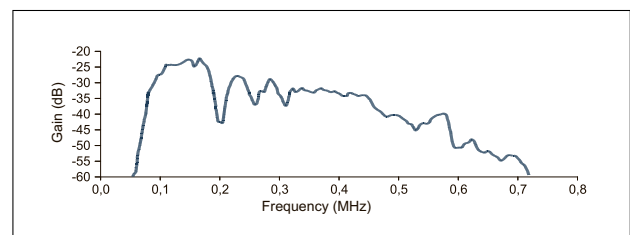


Figure 3. Crystal transducer Physical Acoustics type R15I-AST – frequency response.

means the setup sensitivity of the order 10 pC. In Figure 3 the frequency response is depicted. The sensors were attached to the walls of steel vessel filled with transformer oil.

As the acoustic wave energy attenuation has to be minimized we attached the sensors to metallic vessel walls by magnetic holders and the touching surface of sensors were thoroughly cleaned and smeared with a special contact gel used in ultrasonic diagnostics.

Figure 4 shows the main experimental configuration (a) and setup dimensions (b). The vessel serves as a test device for the measurement with artificial modeled insulation defect and imitates situation in real world high voltage transformer with simplified conditions as described above. The walls have acoustic properties of real h.v. transformers vessel. As an PD source the Böning model [26] was used for continuous and constant PD generation under determined condition see Figure 5. The model has generated PD pulses in gas-filled cavity in similar way as it occurs in h.v. insulation. The spark gap GI was immersed in transformer oil.

The goal of the experiment is to explore the frequency energy shift in given range of acoustic media temperatures. To fulfill it, it is sufficient to apply two acoustic sensors as defect spatial allocation information is neglected [23]. However PD measurement by acoustic method is usually interfered with an ambient noise [27]. Described measurements and experiments were made in laboratory conditions. The measurement setup was adapted to eliminate er-

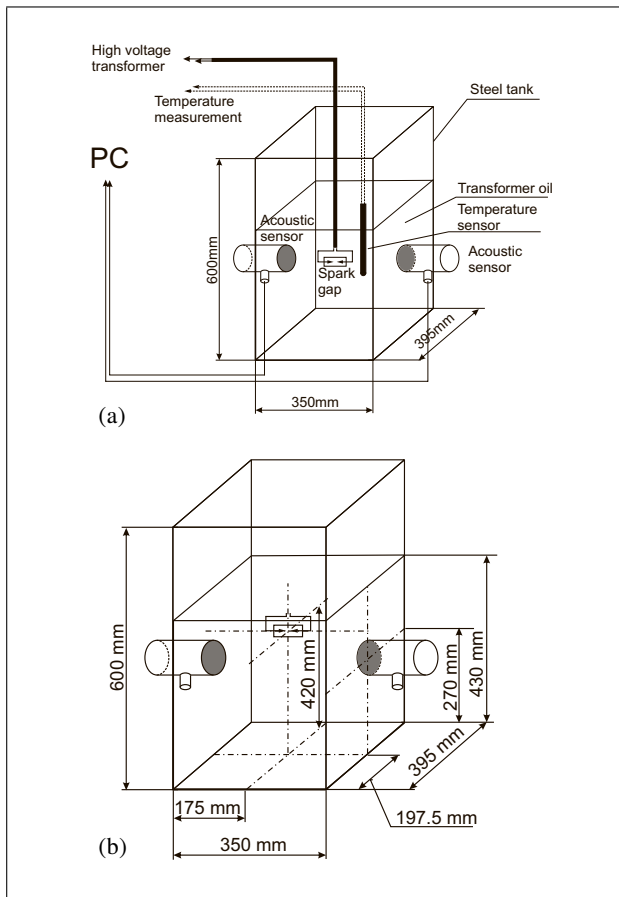


Figure 4. a) Tested object configuration and b) setup dimensions.

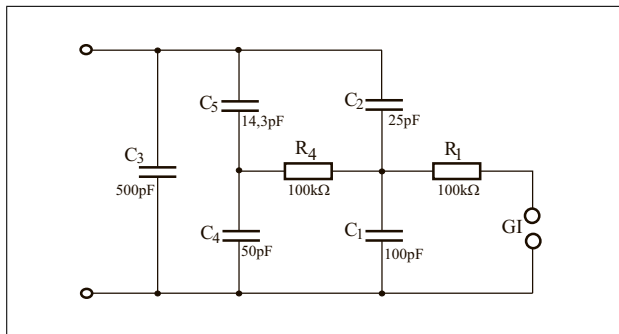


Figure 5. Electrical diagram of adapted Böning model.  $R_1$  and  $R_4$  – resistors,  $C_1$ — $C_5$  – capacitors, GI – spark gap.

rors caused by noisy environment. The timing and thresholding technique was used to cope with the noise problem.

Measurements were made at various temperatures of the transformer oil from 20°C, 40°C, 60°C and 80°C while warming the oil and 80°C, 60°C, 40°C and 20°C while cooling it. This selection corresponds approximately to the temperatures that occur during high voltage electric power device industrial operation conditions.

#### 4. Results and discussion

The aim of the signal analysis was to find relevant parameters for PD characterization which describes changes

Table I. Dominant frequencies and sub-bands.

$T$ (°C)	Dominant Frequency/Sub-band (kHz)
20	125, 160, 240, 280
40	125, 160–175, 225–275, 280, 310–330, 350–360
60	140, 160–180, 230, 266–290, 320, 350, 450
80	75–125, 150–200, 265–285, 300–330, 360, 430–480

Table II. Dominant frequency and sub-band extremes.

Temperature (°C)	Dominant Frequency/Sub-band (kHz)	
	Lowest	Highest
20	100	280
40	125	350–360
60	140	450
80	75–125	430–480

caused by temperature change most evidently. Among the other parameters – e.g. in the time-domain the AE pulse slew rate and time rise, AE hit duration, etc. – the amplitude frequency spectrum appears to be one of the suitable parameters for this purpose.

In Figures 6a to 6d amplitude-frequency spectra are shown for measurements at temperatures of oil in tank beginning from 20°C, 40 °C, 60°C and 80°C with 4.2 kV voltage on electrodes. The input parameter of the analytical and physical model is the temperature of the transformer oil.

For comparison of the frequency shift of amplitude spectrum components to higher frequencies with increasing temperature we calculated amplitude frequency characteristics of a waveform templates. Signal templates in the time domain were calculated by method described in [23] and then Fourier transform was applied on these templates. The main goal of the method is to increase the correlation of specific source waveforms with interpreted signal template in comparison with simple statistical averaging. This is achieved by the waveform time-alignment procedure applied on whole set of recorded signals.

For 20°C dominant frequencies are in the range of 100 kHz, 125 kHz, 160 kHz, 240 kHz and 280 kHz. For temperature 40°C dominant frequencies are shifted to higher values: 125 kHz, 160–175 kHz, 225–275 kHz, 280 kHz, 310–330 kHz and 350–360 kHz.

At 60°C the dominant frequencies are shifted to values 140 kHz, 160–180 kHz, 230 kHz, 266–290 kHz, 320 kHz, 350 kHz and 450 kHz.

During experiments, at highest available temperature of insulating oil the shifts were most obvious. The following dominant frequency sub-bands were calculated: 75–125 kHz, 150–200 kHz, 265–285 kHz, 300–330 kHz, 360 kHz and 430–480 kHz.

The extremes of the dominant frequencies and frequency sub-bands can be deduced from the graphs in Figures 6. The lowest dominant frequency in the case of 20°C was 100 kHz and this is shifted to 125 kHz for 80°C. The highest dominant frequency in the case of 20°C was

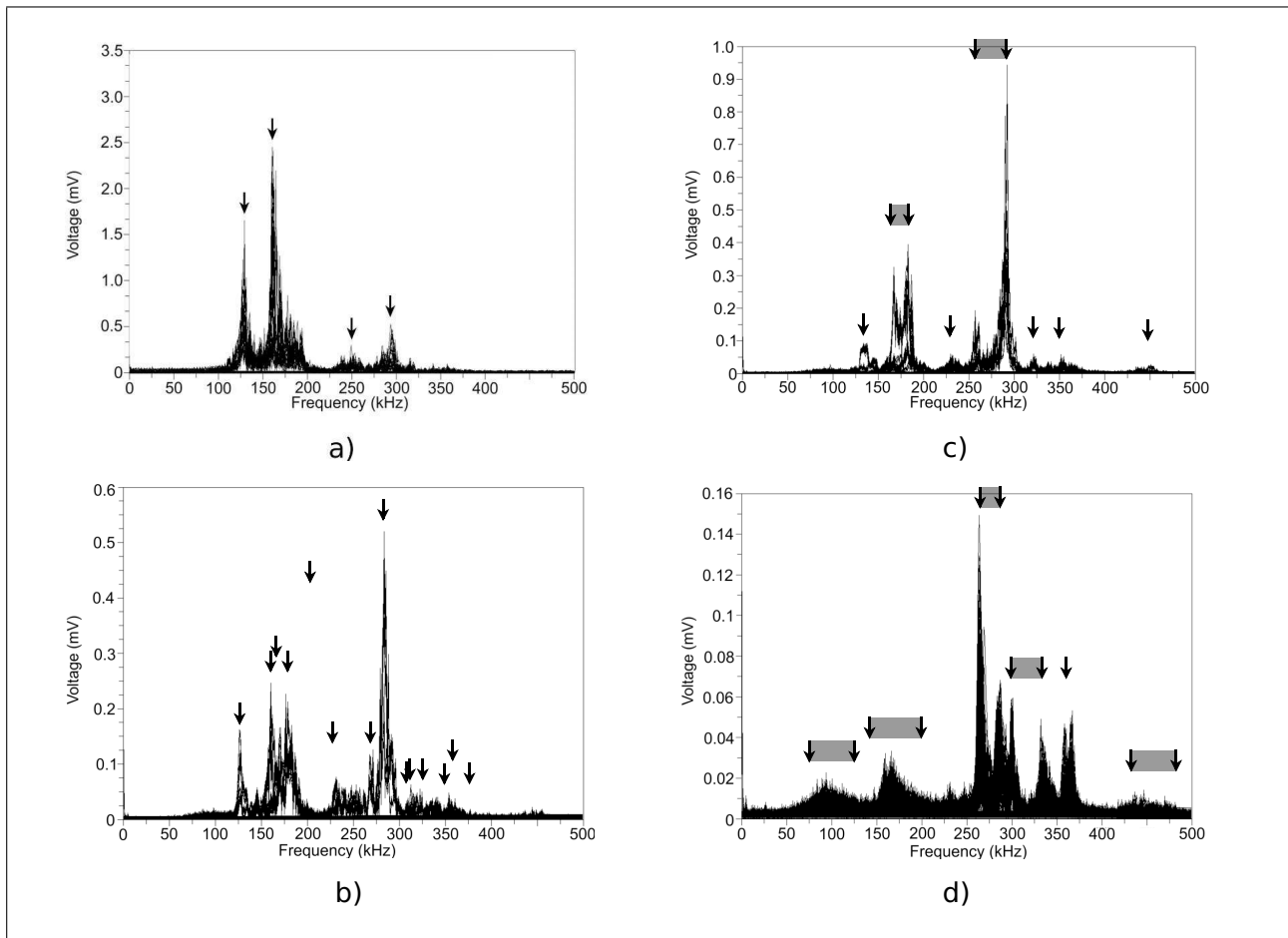


Figure 6. Frequency spectrum overlay at temperature a) 20°C, b) 40°C, c) 60°C, d) 80°C. Dominant frequencies are indicated with arrows.

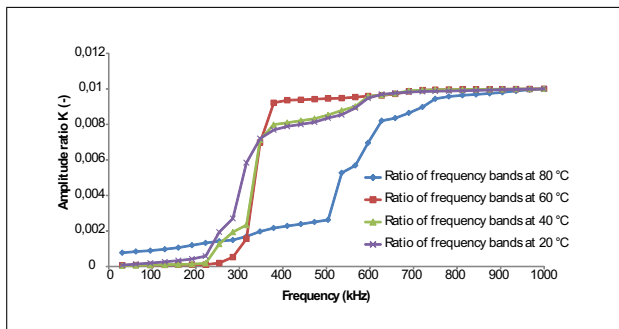


Figure 7. Example of ratio of frequency amplitude sum in 31.25 kHz bands at oil temperatures 20°C, 40°C, 60°C and 80°C.

280 kHz and this is shifted to 480 kHz for 80°C. The overview of calculated values is in Tables I and II respectively.

The analysis of the amplitude component portions is carried out by the application of the formula (8), where the coefficient  $K$  was introduced. The graphical presentation of this ratio can be seen in Figure 7. At lower temperatures i.e. 20°C and 40°C respectively, the  $K$  values indicate higher participation of frequency sub-bands which

begins at 220 kHz and achieve their almost saturated value at 600 kHz.

At oil temperature of 60°C frequency sub-band participation begins at 250–270 kHz and reaches its saturated values at 470 kHz. Therefore the frequency components are concentrated in a narrower band than with other temperatures. At the temperature of 80°C the values of  $K$  begin to raise at 500 kHz and reach saturated values at 800 kHz.

From Figure 7 it is obvious that the lowest frequency sub-bands which significantly participate in the waveform spectra shift to higher values with rising temperature i.e. from 220 kHz to 500 kHz. The highest contributing frequency sub-bands shift from 600 kHz to 800 kHz, which is in both cases a frequency shift of approximately 200 kHz.

## 5. Conclusion

The Acoustic Emission non-destructive technique (NDT) based on the detection and conversion elastic waves to electrical signals and special attention is given to the temperature of physical environment. In the case of proposed method, it has been shown that the temperature causes the frequency shift. This relation could be implemented into

the testing procedure with advantage of temperature influence correction. The interpretation of PD-source type is related to several characteristics and it has been shown that it is influenced by the temperature.

The experiment and the method proposed allow to uncover the effect of acoustic emission energy shift over frequency spectra due to the change of fluid temperature. Higher frequency sub-band participation get more significant at higher temperatures. In the field of non-destructive testing of high voltage power devices it gives new understanding of the temperature role on interpretation of PD generated acoustic emission analysis. As the temperature-frequency relation is not commonly applied in current PD measurement systems, their analytical tools and their decision making procedures can be improved in a way that they will take into consideration the temperature factor. The influence of higher temperatures on shifted signal spectra can help to distinguish between signal markers that are relevant for partial discharge activity detection and evaluation and eliminate markers that are caused by insulating system temperature. This way a better prediction of dangerous PD sources of high voltage power apparatus at various operational conditions can be reached.

Current AE inspection systems capable of PD detection can utilize the information extracted from the change of AE waveform due to temperature. Moreover, presented feature is relative easy implementable into existing AE processing procedure. The AE waveforms properties can be reconsidered more accurate regarding the temperature changes in the object under test.

### Acknowledgement

This work was supported by the Slovak Academy of Sciences in the framework of VEGA 1/0311/15 and Ministry of Education Agency for structural funds of EU in frame of projects No. 26220120055 and 26220220182.

### References

- [1] M. Bassim, M. Dudar, R. Rifaat, R. Roller: Application of acoustic emission for non destructive evaluation of utility inductive reactors. *IEEE Transactions on Power Delivery* **8** (1993) 281–284.
- [2] J. Deng, H. Xiao, W. Huo, M. Luo, R. May, A. Wang, Y. Liu: Optical fiber sensor-based detection of partial discharges in power transformers. *Optics & Laser Technology* **33** (2001) 305–311.
- [3] M. de A. Olivieri, W. Mannheimer, A. Ripper-Neto: On the use of acoustic signals for detection and location of partial discharges in power transformers. *Conference Record of the 2000 IEEE International Symposium on Electrical Insulation, 2000, 2000*, 259–262.
- [4] E. Mohammadi, M. Niroomand, M. Rezaeian, Z. Amini: Partial discharge localization and classification using acoustic emission analysis in power transformer. *Telecommunications Energy Conference, 2009. INTLEC 2009. 31st International, 2009*, 1–6.
- [5] A. Haddad, D. F. Warne: *Advances in high voltage engineering*. The institution of Engineering and Technology, London, UK, 2004.
- [6] P. Toman, M. Paar, J. Orsáč: Possible solutions to problems of voltage asymmetry and localization of failures in mv compensated networks. *IEEE LAUSANNE POWERTECH, 2007, Ecole Polytechnique Federale de Lausanne, 1758–1763*.
- [7] M. Leijon, M. Dahlgren, L. Walfridsson, L. Ming, A. Jaksts: A recent development in the electrical insulation systems of generators and transformers. *IEEE Electrical Insulation Magazine* **17** (2001) 10–15.
- [8] S. Boggs: Partial discharge: overview and signal generation. *IEEE Electrical Insulation Magazine* **6** (1990) 33–39.
- [9] H. Borsi, U. Schroder: Initiation and formation of partial discharges in mineral-based insulating oil. *IEEE Transactions on Dielectrics and Electrical Insulation* **1** (1994) 419–425.
- [10] J. Petras: Partial discharge acoustic emission exploitation. *DISEE 2006, 2006, Slovak University of Technology Bratislava, 96–99*.
- [11] P. Eleftherion: Partial discharge. XXI. acoustic emission based PD source location in transformers. *IEEE Electrical Insulation Magazine* **11** (1995) 22–26.
- [12] T. Boczar, D. Zmarzly: Application of wavelet analysis to acoustic emission pulses generated by partial discharges. *IEEE Transactions on Dielectrics and Electrical Insulation* **11** (2004) 433–449.
- [13] S. Markalous, S. Tenbohlen, K. Feser: Detection and location of partial discharges in power transformers using acoustic and electromagnetic signals. *IEEE Transactions on Dielectrics and Electrical Insulation* **15** (2008) 1576–1583.
- [14] A. Cichon, S. Borucki, T. Boczar, M. Lorenc: Results of the wavelet analysis of the acoustic emission signals generated by partial discharges in insulation oil of various temperature and flow speed. *The European Physical Journal Special Topics* **154** (2008) 31–38.
- [15] J. Zhao, D. Auckland, C. Smith, B. Varlow: Acoustic emission analysis of high voltage insulation. *IEE Proceedings - Science, Measurement and Technology* **146** (1999) 260–263.
- [16] D.-J. Kweon, S.-B. Chin, H.-R. Kwak, J.-C. Kim, K.-B. Song: The analysis of ultrasonic signals by partial discharge and noise from the transformer. *IEEE Transactions on Power Delivery* **20** (2005) 1976–1983.
- [17] J. Lubbers, R. Graaff: A simple and accurate formula for the sound velocity in water. *Ultrasound in Medicine and Biology* **24** (1998) 1065–1068.
- [18] L. Lundgaard: Partial discharge. XIII. acoustic partial discharge detection-fundamental considerations. *IEEE Electrical Insulation Magazine* **8** (1992) 25–31.
- [19] A. Krivda: Automated recognition of partial discharges. *IEEE Transactions on Dielectrics and Electrical Insulation* **2** (1995) 796–821.
- [20] R. Harrold: Acoustical technology applications in electrical insulation and dielectrics. *IEEE Transactions on Electrical Insulation* **EI-20** (1985) 3–19.
- [21] Z. Skvor: *Akustika a elektroakustika*. Academia, Praha, 2001.
- [22] X. Wang, B. Li, Z. Xiao, O. L. Russo, H. Roman, K. Chin, K. R. Farmer: Acoustic energy shifting in transformer oil at different temperatures. *IEEE Transactions on Power Delivery* **20** (2005) 2356–2357.
- [23] J. Petras: Defective insulation localization in electric power devices by acoustic methods. *Technical University of Kosice, 2008*.
- [24] H. Zhang, T. R. Blackburn, B. T. Phung, D. Sen: A novel wavelet transform technique for on-line partial discharge

- measurements. 1. WT de-noising algorithm. Dielectrics and Electrical Insulation, IEEE Transactions on **14** (2007) 3–14.
- [25] A. Pollock: Acoustic emission inspection. PCI-2 based AE system, rev. 2, 2004, Physical Acoustic Corporation, 1–15.
- [26] W. Böning: Luftgehalt und Luftspaltverteilung geschichteter Dielektrika. I: Untersuchung der Entladungen in einzelnen Luftspalten bei äußerem Wechselfeld. Archiv für Elektrotechnik **48** (1963) 7–22.
- [27] J. F. Douglas: Fluid mechanics. Pearson Education, 2005.